

Three-Dimensional Energy Transfer in Space Plasma Turbulence from Multipoint Measurement

Francesco Pecora^{1,*}, Yan Yang¹, William H. Matthaeus¹, Alexandros Chasapis², Kristopher G. Klein³, Michael Stevens⁴, Sergio Servidio⁵, Antonella Greco⁵, Daniel J. Gershman⁶, Barbara L. Giles⁶, and James L. Burch⁷

¹Department of Physics and Astronomy, University of Delaware, Newark, Delaware 19716, USA

²Laboratory for Atmospheric and Space Physics, University of Colorado Boulder, Boulder, Colorado 80309, USA


³Lunar and Planetary Laboratory, University of Arizona, Tucson, Arizona 85721, USA

⁴Center for Astrophysics, Harvard and Smithsonian, Cambridge, Massachusetts 02138, USA

⁵Dipartimento di Fisica, Università della Calabria, I-87036 Cosenza, Italy

⁶NASA Goddard Space Flight Center, Greenbelt, Maryland 20771, USA

⁷Southwest Research Institute, San Antonio, Texas 78238, USA

 (Received 3 July 2023; revised 20 September 2023; accepted 26 October 2023; published 28 November 2023)

A novel multispacecraft technique applied to Magnetospheric Multiscale Mission data in the Earth's magnetosheath enables evaluation of the energy cascade rate from the full Yaglom's equation. The method differs from existing approaches in that it (i) is inherently three-dimensional, (ii) provides a statistically significant number of estimates from a single data stream, and (iii) allows visualization of energy flux in turbulent plasmas. This new “lag polyhedral derivative ensemble” technique exploits ensembles of tetrahedra in lag space and established curlometerlike algorithms.

DOI: [10.1103/PhysRevLett.131.225201](https://doi.org/10.1103/PhysRevLett.131.225201)

Introduction.—A long-standing problem in turbulence is how energy is transferred across scales from large-scale reservoirs to dissipation. The problem relates to fluids and plasmas throughout the Universe, but until recent decades was studied almost exclusively in the hydrodynamic context. Experimental studies have always been crucial in the development of the subject [1,2], but until now a full three-dimensional evaluation of the Yaglom cascade rate has not been accomplished (for a review, see [3]). Evaluating this fundamental quantity is hindered by its inherently three-dimensional and scale-dependent nature, while, as yet, multiscale multipoint measurements have not been available in space missions. We present such an evaluation below, using data from the Magnetosphere Multiscale Mission (MMS) in the terrestrial magnetosheath.

de Kármán and Howarth [4] provided seminal results that describe turbulence in terms of double and triple correlations of fluctuations, indicating a balance between time dependence, nonlinear transfer, and dissipation. Based on the von Kármán-Howarth (vKH) equations, Kolmogorov [5] derived an exact relation between the third-order structure function and the rate at which energy is “cascaded” through scales. Later, Yaglom [6] derived a similar expression for a passive scalar (temperature) in turbulence involving mixed velocity-temperature third-order structure function. These results were derived for homogeneous isotropic incompressible hydrodynamics.

Politano and Pouquet [7,8] generalized the hydrodynamic results to incompressible magnetohydrodynamics (MHD), a model often adopted as a good description of

space plasmas [9]. They extend the vKH equation to include the properties of a magnetized fluid described by the Elsässer fields $\mathbf{z}^\pm = \mathbf{v} \pm \mathbf{b}$, where \mathbf{v} is the velocity and \mathbf{b} the magnetic field in Alfvén units—normalized to $\sqrt{4\pi n_p m_p}$ for proton number density n_p and mass m_p . The main result is a relation analogous to Kolmogorov's “4/5 law” [5] in the framework of homogeneous isotropic magnetized fluids. However, for anisotropic systems, typical of space plasmas, the isotropic assumption can lead to biased results. Here, we will use the MHD energy evolution equation with fully three-dimensional lag-space differential operators, thus avoiding the isotropy assumption when calculating the energy dissipation rate. The vKH equation for MHD reads

$$\frac{\partial}{\partial t} \langle |\delta \mathbf{z}^\pm|^2 \rangle = -\nabla_\ell \cdot \langle \delta \mathbf{z}^\mp |\delta \mathbf{z}^\pm|^2 \rangle + 2\nu \nabla_\ell^2 \langle |\delta \mathbf{z}^\pm|^2 \rangle - 4\epsilon^\pm \quad (1)$$

for kinematic viscosity ν . The Elsässer increments at vector lag ℓ are $\delta \mathbf{z}^\pm(\ell) = \mathbf{z}^\pm(\mathbf{x}) - \mathbf{z}^\pm(\mathbf{x} + \ell)$. Derivatives ∇_ℓ are in lag space and ϵ^\pm is the energy dissipation (or cascade) rate. In a turbulent plasma, one can roughly distinguish three regimes: (i) the energy-containing range, where the energy is provided to the system from the largest structures; (ii) the dissipation range, where energy is eventually dissipated at very small scales; and (iii) the inertial range, at intermediate scales, through which energy is transferred (“cascades”) from the injection to dissipation scales.

The time-varying term on the left-hand side of Eq. (1) usually dominates at very large spatial scales; the nonlinear term—the first on the right-hand side—peaks at separations that fall into the inertial range; and the dissipative term—the second on the right-hand side—becomes important at very small spatial scales. The sum of these terms is proportional to the mean dissipation rate [10–13]. For sufficient separations between injection and dissipation scales, each term in Eq. (1) is dominant over a range of scales in which the others are negligible. This condition is usually associated with high Reynolds numbers or, equivalently, very large systems. For lower Reynolds numbers (e.g., in simulations), scale separation is not pristine, and different contributions “leak” into neighboring scale ranges. In this case, the evaluation of each term gives a partial cascade rate estimate as it misses contributions from the other terms at those scales.

When applying this theory to *in situ* spacecraft observations, the time derivative term is inaccessible since spacecraft do not follow the flow [14]. The dissipative term requires knowledge of underlying dissipative mechanisms, e.g., viscosity or Joule heating, which itself is a separate problem, especially for noncollisional plasmas [15–17]. Therefore, here, we focus on the nonlinear term and the relationship

$$\nabla_{\ell} \cdot \langle \delta \mathbf{z}^{\mp} |\delta \mathbf{z}^{\pm}|^2 \rangle = -4\epsilon^{\pm}, \quad (2)$$

which involves a mixed third-order structure function. By analogy with [6], $\langle \delta \mathbf{z}^{\mp} |\delta \mathbf{z}^{\pm}|^2 \rangle = \mathbf{Y}^{\pm}$ is called Yaglom flux, and $\nabla_{\ell} \cdot \mathbf{Y}^{\pm} = -4\epsilon^{\pm}$ Yaglom’s law. The total dissipation rate is $\epsilon = (\epsilon^+ + \epsilon^-)/2$. Equation (2) applies to anisotropic systems since vKH is derived without assuming isotropy. The terms in Eq. (1) overlap for incomplete scale separation or if available lags are not in the inertial range. Then, Eq. (2) provides a partial answer, interpreted as the contribution to the total energy cascade rate from the nonlinear term only.

Most previous (partial) cascade rate measurements in space plasmas are limited to directional averages [18,19], a combination of 2D + 1D models [20,21] or, the 1D isotropic version of Eq. (2) [22–26]. Recent numerical

studies [10,13,27] showed that the directional dependence of Yaglom’s equation is not negligible when a large-scale magnetic field is present [even though such a field does not appear in Eq. (1); see [28]]. Therefore, isotropy is not a good assumption, and instead, one requires measurements in several directions in 3D lag space. Currently, as far as we know, direct observations of the behavior of the full Yaglom flux vector in anisotropic systems have been conducted only in fluid experiments [29] and numerical simulations [10]. It is known, for example, that an anisotropic system has different extensions of the inertial range in different directions [10,27,30,31]. A more comprehensive description of turbulence can be obtained by studying the Yaglom flux vector through which it is possible to characterize the inertial range in various directions, thus quantifying the degree of anisotropy. Below, we implement a technique that enables numerous calculations of the lag-space divergence in Eq. (2), thus obtaining a statistical evaluation of the cascade rate.

Data.—We use data from MMS [32] for the magnetic field from the fluxgate magnetometers [33], proton velocity, and electron density from the Fast Plasma Investigation [34]. Measurements are available in burst mode at cadences of 128 Hz, 150 ms, and 30 ms, respectively. For velocities, spintone has been removed; the magnetic field data is already despun by the mission. We use the electron density, as it generally is more accurately determined, and assume quasineutrality. Density signals have been checked not to have values larger than 50 cm^{-3} that can be polluted by instrumental inaccuracies. All data have been resampled to the lowest common cadence of 150 ms. We analyzed several intervals from [35] during which MMS was in the magnetosheath. Properties of these intervals, such as the magnetic and density fluctuations, ion plasma beta (ratio of thermal to magnetic pressures), correlation lengths and times, and ion inertial length, are listed in Table I, including their mean turbulence cascade rates calculated using the lag polyhedral derivative ensemble (LPDE) technique described below.

Technique.—We implemented the LPDE technique described in [31] through which it is possible to have several estimates of the cascade rate using Yaglom’s law,

TABLE I. Reported are the dates and times of the analyzed intervals, magnetic $\delta b/B$ and density $\delta\rho/\rho$ fluctuation levels (r.m.s. over mean), proton plasma beta β (ratio between thermal and magnetic pressure), correlation time τ_c and length λ_c [36], ion inertial length d_i , and the mean energy cascade rate ϵ obtained from the LPDE technique, with associated uncertainties calculated as the standard deviation of their respective histograms.

	Date (UTC)	$\delta b/B$	$\delta\rho/\rho$	β	τ_c (s)	λ_c (km)	d_i (km)	$\langle \epsilon \rangle$ ($10^6 \text{ J kg}^{-1} \text{ s}^{-1}$)
I	2017-09-28 06:31:33–07:01:43	0.51	0.19	5.9	81.0	41229	46	-1.5 ± 0.8
II	2017-11-10 22:35:43–22:52:03	3.17	0.43	8.3	2.9	1377	74	22.5 ± 9.5
III	2017-12-21 07:21:54–07:48:01	1.92	0.31	4.7	6.1	652	50	24.8 ± 13.4
IV	2017-12-26 06:12:43–06:52:23	0.82	0.21	4.5	16.3	3712	48	1.6 ± 0.4
V	2018-04-19 05:10:23–05:41:53	2.99	0.29	15.0	5.1	1168	36	1.9 ± 0.7

Eq. (2). The technique is based on the fact that derivatives have to be computed in lag space to evaluate Yaglom's equation. Each pair of spacecraft i, j is separated by a vector baseline $\boldsymbol{\ell} = \mathbf{r}_{ij} = \mathbf{r}_i - \mathbf{r}_j$, where \mathbf{r}_i is the position of the i th spacecraft. Using MMS, we have four spacecraft connected by six vector baselines, thus we can compute six values of the increment $\delta \mathbf{z}_{ij}(\mathbf{r}_{ij}) = \mathbf{z}_i(\mathbf{r}_i) - \mathbf{z}_j(\mathbf{r}_j)$, where $i, j = 1, \dots, 4, i < j$.

Previously, the LPDE technique was tested using simulations and nine HelioSwarm-like spacecraft trajectories. Here, the method is applied for the first time to real data using MMS, with few improvements that provide a larger pool of estimates.

In order to increase the number of estimates for the dissipation rate, we notice that the choice of the order of the pair is arbitrary, and, therefore, we can have additional six points in lag space by just reversing the order of the pairs, namely using $j, i = 1, \dots, 4, j < i$. It means that we will have a total of 12 points in lag space with $\delta \mathbf{z}_{ji} = -\delta \mathbf{z}_{ij}$. Of course, these additional points will not give independent information but will be valuable in the construction of tetrahedra as we will describe below.

Since we want to use algorithms that have been well-tested using MMS data in the past, e.g., the curlometer [37], we examine only tetrahedral configurations, that is, we rearrange our points in lag space in sets of four. The number of nonrepeating partitions of K elements out of N total elements is given by $C_N^K = \binom{N}{K} = [N! / K!(N - K)!]$. If we were to use the six points in lag space that come from $\delta \mathbf{z}_{ij}(\mathbf{r}_{ij})$, we would have $C_6^4 = \binom{6}{4} = 15$ possible tetrahedra. When we add $\delta \mathbf{z}_{ji}(\mathbf{r}_{ji})$, our available points become 12, with a total of $C_{12}^4 = \binom{12}{4} = 495$ tetrahedra. Evidently, not all configurations are independent.

Indeed, an identical tetrahedron can be built using any four points and their reflections. We discarded the solutions that are obtained from these redundant identical tetrahedra. Moreover, some configurations, those that are composed of two points and their reflections, have their barycenter coinciding with the origin. These tetrahedra would provide an estimate of the cascade rate at zero lag, which is irrelevant. Their number is $C_6^2 = \binom{6}{2} = 15$. The total number of independent estimates of Eq. (2) is therefore $\frac{1}{2}(C_{12}^4 - C_6^2) = 240$.

We also need to consider the quality of the tetrahedral shape, which can affect the accuracy of the calculation of the divergence, and therefore, impact the resulting estimate of the dissipation rate. Indeed, well-behaved real-space configurations (close in shape to a regular tetrahedron) do not necessarily translate into well-behaved lag-space tetrahedra. For the quality check of the 240 independent tetrahedra in lag space, we make use of the elongation-planarity parameters described in Paschmann and Daly [38]. We compute the volumetric tensor in lag space $L_{jk} = (1/N) \sum_{\alpha=1}^N (\ell_{\alpha j} \ell_{\alpha k} - \ell_{\alpha j} \ell_{\alpha k})$, where $\ell_{\alpha j}$ is the j th component of the vertex α . Averaging these over the

vertices gives the j th component of the mesocenter, $\ell_{bj} = \langle \ell_{\alpha j} \rangle_{\alpha}$. We use $N = 4$. Calculating the three eigenvalues of the volumetric tensor, $\lambda_1 \geq \lambda_2 \geq \lambda_3$, we can define elongation (E) and planarity (P) parameters as $E = 1 - \sqrt{\lambda_2/\lambda_1}$ and $P = 1 - \sqrt{\lambda_3/\lambda_2}$, respectively. We will consider suitable for our analysis all tetrahedra constrained in a certain region of the EP plane defined by the distance parameter $d_{EP} = \sqrt{E^2 + P^2}$. We initially use only results obtained from lag tetrahedra such that $d_{EP} \leq 0.6$. For these, the errors should be smaller than 20% (see p. 408 of Paschmann and Daly [38]). Additionally, this threshold automatically rejects tetrahedra that are nearly planar or collinear.

Results.—We computed the Yaglom flux Y^{\pm} using the 12 available MMS baselines as described in the previous section. We evaluate the divergence by selecting the 12 points in lag space, in subsets of four, covering all possible 240 independent lag tetrahedra. This procedure has been applied to all intervals listed in Table I. Since the results are qualitatively similar, here we show those pertaining to interval IV (December 26, 2017). After estimating the cascade rate using lag tetrahedra in the region of the EP plane defined as $d_{EP} \leq 0.6$, we gradually increase the threshold to $d_{EP}^* \leq 0.85$, verifying that this procedure does not affect the results to the precision that we report. By doing so, the number of estimates increases from 27 to 134 and therefore we decided to keep the larger number of available points for statistical purposes. In Fig. 1, we report the elongation and planarity values for the lag tetrahedra, together with the chosen threshold $d_{EP}^* = 0.85$ and the initial reference threshold $d_{EP} = 0.6$. Tetrahedra in lag space give a rather uniform coverage of the EP plane, with a few points at $P = 1$ indicating flat geometries.

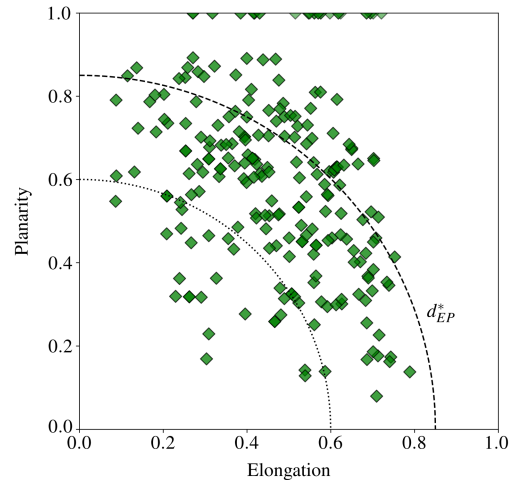


FIG. 1. Geometrical characteristics for lag tetrahedra. The dashed line indicates the threshold $d_{EP}^* = \sqrt{E^2 + P^2} = 0.85$. Lag tetrahedra with $d_{EP} \leq d_{EP}^*$ are used for further analysis, and the others are discarded. For reference, we also indicated the threshold at $d_{EP} = 0.6$ with a dotted line.

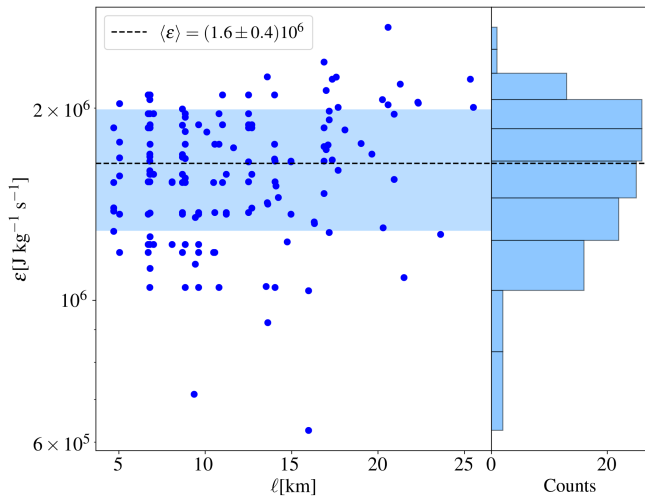


FIG. 2. Scatter plot of the cascade rate as a function of lag tetrahedra mesocenter position. On the side, the histogram of the results is reported. The horizontal black dashed line indicates the average of the histogram, and the blue shaded region represents the variability around the mean.

As an additional convergence test, we added random noise with a flat distribution to the data time series. For different quantities, we used different amplitudes to mimic instrumental uncertainties [39]. Specifically, the imposed uncertainties range for density and velocity from 5% to 25%, and 0.05–0.2 nT for the magnetic field. Even when all uncertainties are set at their maximum amplitude, the results are within the errors of the estimated values with the original time series, confirming the robustness of LPDE.

In solving Yaglom’s equation, each estimated value of the cascade rate is assigned to the increment corresponding to the mesocenter of the lag tetrahedron that is used to compute the divergence. The scatter plot of the values of the cascade rate as a function of the amplitude of the mesocenter $|\ell|$ in lag space is shown in Fig. 2. A visualization of some of the lag tetrahedra used to compute the divergence is given in Fig. 3(a).

From the average, the value that we obtain for the cascade rate is $\langle \epsilon \rangle = (1.6 \pm 0.4) 10^6 \text{ J kg}^{-1} \text{ s}^{-1}$. The quoted uncertainty is the standard deviation about the mean of the measured distribution. The values obtained for the cascade rates are comparable to those in the literature [19]. However, the present results are more robust since we have not assumed isotropy [13], and the large number of estimates per interval allows consideration of the signed value [40]. Indeed, for some intervals, even if the majority of the estimates are positive, we find a few that are negative. This suggests that additional care is needed when only single estimates are available. An isolated negative value may be nonrepresentative and provide misleading interpretations, e.g., invoking inverse cascade processes. In general, increasing the number of observation positions

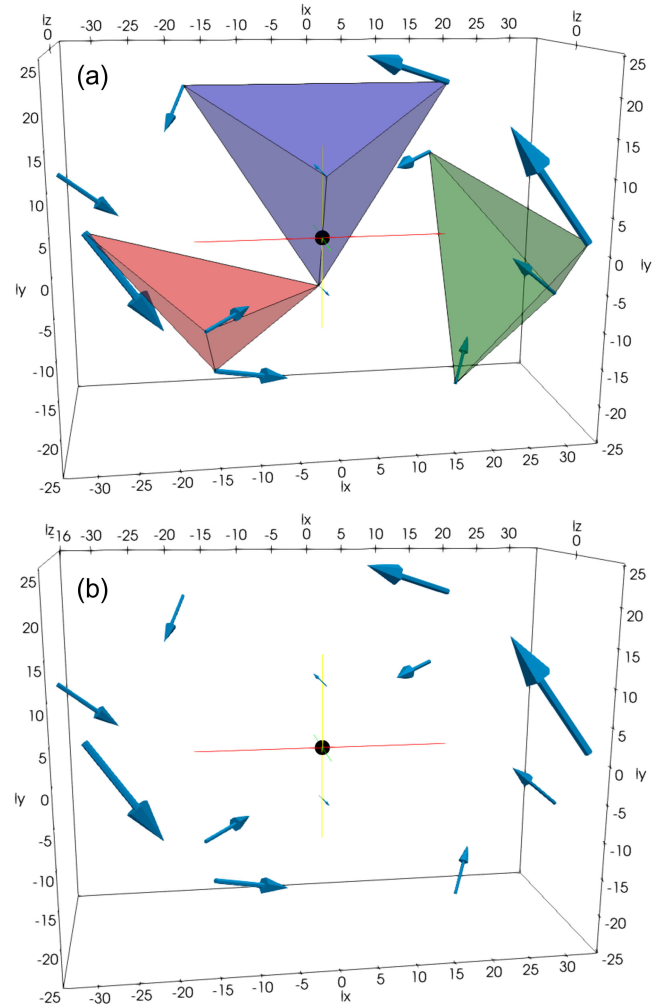


FIG. 3. (a) Yaglom flux vectors in lag space with some tetrahedra, over which Yaglom’s law is solved (shaded volumes). (b) Same plot without highlighted tetrahedra. It is possible to appreciate the swirling motion of the Yaglom flux pointing toward the origin (indicated by the black sphere).

decreases error. This will be the case when using the present method in future multispacecraft missions. For implementation in numerical simulations, see [31].

Another quantity that is of physical interest is the Yaglom flux itself $\mathbf{Y} = [(\mathbf{Y}^+ + \mathbf{Y}^-)/2]$, as it is related to the nonlinear transfer of energy across scales. For a homogeneous, isotropic system, one expects the Yaglom flux to have magnitudes proportional to the distance from the origin and radially pointing toward it. Previous numerical studies [10] provided a picture of how the Yaglom flux behaves in lag space. In particular, it was confirmed that \mathbf{Y} is larger in magnitude further from the origin and, when the system is anisotropic, it shows some deflections from the radial trend. In space plasmas, it has not been possible to visualize the behavior of the Yaglom flux prior to the development of the LPDE technique.

From the present results, we know the flux vector at six (12) points in lag space and can examine its behavior, as shown in Fig. 3(b). This visualization of the Yaglom flux using space data confirms the expected basic features. The arrows' lengths in the figure are proportional to the magnitude of the Yaglom flux, and we notice that they become smaller as they approach the origin of the system where dissipation will eventually deal with the energy that has been transferred there. Moreover, we observe a swirling of the arrows around the origin, instead of radially pointing toward it as it would if turbulence was isotropic.

Discussion and conclusions.—We applied the novel LPDE multispacecraft technique, Pecora *et al.* [31], to MMS measurements in the magnetosheath to evaluate the turbulence cascade rate due to Yaglom's term in the vKH equation. The technique is here extended by exploiting the symmetry properties of the mixed third-order structure function. This provides a statistically significant (> 100) number of estimates of the cascade rate by computing the full divergence in Eq. (2). Moreover, we are also able to visualize, for the first time in space plasmas, the Yaglom flux vector that is responsible for transferring energy toward smaller scales from the inertial range.

Previously, cascade rate estimation in space plasmas has been limited to one value per interval and mostly employing a 1D version of Yaglom's equation [e.g., [3,22]]. This approximation, however, assumes isotropy, as well as the usage of Taylor's hypothesis, which convolves space and time correlations.

Anisotropy has an effect on the direction of the Yaglom flux \mathbf{Y} in both fluid experiments [29] and plasma simulations [10]. When a mean magnetic field is present, \mathbf{Y} tilts toward the plane perpendicular to the direction of the field. Therefore, the directionality of \mathbf{Y} is a measure of anisotropy. In solar wind, third-order structure functions have been used to obtain cascade rates employing Taylor hypothesis and an isotropic or two-dimensional (2D) plus 1D paradigm [3,20–22]. In numerical simulations, it was shown that the isotropic assumption can provide imprecise cascade rates, and variability due to directional sampling can be an order of magnitude or more [10,13,27]. Improved results are obtained when both the parallel and perpendicular components of \mathbf{Y} are considered [10,20,21]. These former studies, along with the present results, confirm that the full vectorial nature of \mathbf{Y} must be taken into account to obtain realistic estimates.

Another important issue is statistical convergence. When single point estimates are employed, one may require many samples, possibly spanning years, for convergence of cascade estimates [21]. In that case, the ensemble is highly nonlocal and does not characterize a single time period. By providing many estimates in a single sample, the present method avoids this complication.

In this work, we observe features of the Yaglom flux that have never been observed in space plasmas before and that agree with fluid experiments [29] and numerical simulations [10]. We see that (i) Y magnitudes become smaller when approaching smaller scales where energy is eventually dissipated, and (ii) the tilting of the flux vectors, a departure from the often-assumed radial convergence, possibly due to the anisotropy of the system.

A point to emphasize is that the MMS mission provides lags that are smaller than the inertial scale and therefore, albeit precise, this is a partial evaluation of the full energy cascade rate that would require the computation of all terms in the vKH equation.

Another important concept to address is the scale dependence of the dissipation rate. If one could measure all terms exactly, the dissipation rate would be constant across scales [11–13]. However, different contributions appear to be dominant at different scales. The precision required to compute the divergence in Yaglom's law does not allow the usual implementation of Taylor's hypothesis. This restriction results in a limited range of accessible scales as shown in Fig. 2. In particular, we find tetrahedra spanning scales for about half of a decade and therefore decided to provide an average value within this interval rather than forcing a scaling law. The result, although partial, sets a lower limit to the value of the total dissipation rate.

Current space missions do not allow for a complete evaluation of the total cascade rate, which is composed of several channels. Commonly addressed are compressible [40] and Hall [11,41] corrections that require additional assumptions (e.g., isothermal equation of state [42]). In this Letter, we focused on the nonlinear contribution of the incompressible channel that does not require further assumptions.

The present result advances multispacecraft techniques for measurement of anisotropic turbulence properties in space plasmas [30,38,43]. We (i) eliminate reliance on the Taylor hypothesis, (ii) obtain the cascade rate with no assumption of rotational symmetry, and (iii) provide a statistically significant number of estimates using even short intervals. The technique may be applied to theories of energy conversion that include compressibility, Hall, and other kinetic effects not considered here.

Current limitations such as restrictions to the magnetosheath and to scales smaller than the inertial range will be overcome once the next generation of multiscale multispacecraft missions, such as HelioSwarm [44,45] and Plasma Observatory [46], appear in the solar wind.

F. P. thanks S. Oughton for his useful comments. Supported by NASA MMS under Grant No. 80NSSC19K0565 at the University of Delaware and 80NSSC21K0454, 80NSSC22K0688 grants at the University of Colorado Boulder. K.G.K. was supported by NASA Contract No. 80ARC021C0001.

*Corresponding author: fpecora@udel.edu

- [1] A. S. Monin and A. M. Yaglom, *Statistical Fluid Mechanics, Vols 1 and 2* (MIT Press, Cambridge, 1971, 1975).
- [2] S. B. Pope, *Turbulent Flows* (Cambridge University Press, Cambridge, 2000).
- [3] R. Marino and L. Sorriso-Valvo, Scaling laws for the energy transfer in space plasma turbulence, *Phys. Rep.* **1006**, 1 (2023), scaling laws for the energy transfer in space plasma turbulence.
- [4] T. de Karman and L. Howarth, On the statistical theory of isotropic turbulence, *Proc. R. Soc. A* **164**, 192 (1938).
- [5] A. N. Kolmogorov, Dissipation of energy in the locally isotropic turbulence, *Proc. Math. Phys. Sci.* **434**, 15 (1941).
- [6] A. Yaglom, On the local structure of a temperature field in a turbulent flow, *Dokl. Akad. Nauk SSSR* **69**, 743 (1949), https://archive.org/details/nasa_techdoc_19880069107/mode/2up.
- [7] H. Politano and A. Pouquet, Dynamical length scales for turbulent magnetized flows, *Geophys. Res. Lett.* **25**, 273 (1998).
- [8] H. Politano and A. Pouquet, von Kármán–Howarth equation for magnetohydrodynamics and its consequences on third-order longitudinal structure and correlation functions, *Phys. Rev. E* **57**, R21 (1998).
- [9] A. Barnes, Hydromagnetic waves and turbulence in the solar wind, in *Solar System Plasma Physics*, edited by E. N. Parker, C. F. Kennel, and L. J. Lanzerotti (North-Holland, Amsterdam, 1979), Vol. I, p. 251.
- [10] A. Verdini, R. Grappin, P. Hellinger, S. Landi, and W. C. Müller, Anisotropy of third-order structure functions in MHD turbulence, *Astrophys. J.* **804**, 119 (2015).
- [11] P. Hellinger, A. Verdini, S. Landi, L. Franci, and L. Matteini, von Kármán–Howarth equation for hall magnetohydrodynamics: Hybrid simulations, *Astrophys. J. Lett.* **857**, L19 (2018).
- [12] Y. Yang, W. H. Matthaeus, S. Roy, V. Roytershteyn, T. N. Parashar, R. Bandyopadhyay, and M. Wan, Pressure—strain interaction as the energy dissipation estimate in collisionless plasma, *Astrophys. J.* **929**, 142 (2022).
- [13] Y. Wang, R. Chhiber, S. Adhikari, Y. Yang, R. Bandyopadhyay, M. A. Shay, S. Oughton, W. H. Matthaeus, and M. E. Cuesta, Strategies for determining the cascade rate in mhd turbulence: Isotropy, anisotropy, and spacecraft sampling, *Astrophys. J.* **937**, 76 (2022).
- [14] G. I. Taylor, The spectrum of turbulence, *Proc. R. Soc. A* **164**, 476 (1938).
- [15] Y. Yang, W. H. Matthaeus, T. N. Parashar, C. C. Haggerty, V. Roytershteyn, W. Daughton, M. Wan, Y. Shi, and S. Chen, Energy transfer, pressure tensor, and heating of kinetic plasma, *Phys. Plasmas* **24**, 072306 (2017).
- [16] D. Verscharen, K. G. Klein, and B. A. Maruca, The multi-scale nature of the solar wind, *Living Rev. Solar Phys.* **16**, 5 (2019).
- [17] O. Pezzi, H. Liang, J. L. Juno, P. A. Cassak, C. L. Vásconez, L. Sorriso-Valvo, D. Perrone, S. Servidio, V. Roytershteyn, J. M. TenBarge, and W. H. Matthaeus, Dissipation measures in weakly collisional plasmas, *Mon. Not. R. Astron. Soc.* **505**, 4857 (2021).
- [18] K. T. Osman, M. Wan, W. H. Matthaeus, B. Breech, and S. Oughton, Directional alignment and non-Gaussian statistics in solar wind turbulence, *Astrophys. J.* **741**, 75 (2011).
- [19] R. Bandyopadhyay, A. Chasapis, R. Chhiber, T. N. Parashar, W. H. Matthaeus, M. A. Shay, B. A. Maruca, J. L. Burch, T. E. Moore, C. J. Pollock, B. L. Giles, W. R. Paterson, J. Dorelli, D. J. Gershman, R. B. Torbert, C. T. Russell, and R. J. Strangeway, Incompressible energy transfer in the earth’s magnetosheath: Magnetospheric multiscale observations, *Astrophys. J.* **866**, 106 (2018).
- [20] B. T. MacBride, C. W. Smith, and M. A. Forman, The turbulent cascade at 1 au: Energy transfer and the third-order scaling for mhd, *Astrophys. J.* **679**, 1644 (2008).
- [21] J. E. Stawarz, C. W. Smith, B. J. Vasquez, M. A. Forman, and B. T. MacBride, The turbulent cascade and proton heating in the solar wind at 1 au, *Astrophys. J.* **697**, 1119 (2009).
- [22] L. Sorriso-Valvo, R. Marino, V. Carbone, A. Noullez, F. Lepreti, P. Veltri, R. Bruno, B. Bavassano, and E. Pietropaolo, Observation of inertial energy cascade in interplanetary space plasma, *Phys. Rev. Lett.* **99**, 115001 (2007).
- [23] V. Carbone, R. Marino, L. Sorriso-Valvo, A. Noullez, and R. Bruno, Scaling laws of turbulence and heating of fast solar wind: The role of density fluctuations, *Phys. Rev. Lett.* **103**, 061102 (2009).
- [24] L. Z. Hadid, F. Sahraoui, and S. Galtier, Energy cascade rate in compressible fast and slow solar wind turbulence, *Astrophys. J.* **838**, 9 (2017).
- [25] R. Bandyopadhyay, L. Sorriso-Valvo, A. Chasapis, P. Hellinger, W. H. Matthaeus, A. Verdini, S. Landi, L. Franci, L. Matteini, B. L. Giles, D. J. Gershman, T. E. Moore, C. J. Pollock, C. T. Russell, R. J. Strangeway, R. B. Torbert, and J. L. Burch, In situ observation of hall magnetohydrodynamic cascade in space plasma, *Phys. Rev. Lett.* **124**, 225101 (2020).
- [26] N. Andrés, F. Sahraoui, S. Huang, L. Z. Hadid, and S. Galtier, The incompressible energy cascade rate in anisotropic solar wind turbulence, *Astron. Astrophys.* **661**, A116 (2022).
- [27] B. Jiang, C. Li, Y. Yang, K. Zhou, W. H. Matthaeus, and M. Wan, Energy transfer and third-order law in forced anisotropic MHD turbulence with hyperviscosity, *J. Fluid Mech.* **974**, A20 (2023).
- [28] M. Wan, W. H. Matthaeus, H. Karimabadi, V. Roytershteyn, M. Shay, P. Wu, W. Daughton, B. Loring, and S. C. Chapman, Intermittent dissipation at kinetic scales in collisionless plasma turbulence, *Phys. Rev. Lett.* **109**, 195001 (2012).
- [29] C. Lamriben, P.-P. Cortet, and F. Moisy, Direct measurements of anisotropic energy transfers in a rotating turbulence experiment, *Phys. Rev. Lett.* **107**, 024503 (2011).
- [30] F. Sahraoui, M. L. Goldstein, G. Belmont, P. Canu, and L. Rezeau, Three dimensional anisotropic k spectra of turbulence at subproton scales in the solar wind, *Phys. Rev. Lett.* **105**, 131101 (2010).
- [31] F. Pecora, S. Servidio, L. Primavera, A. Greco, Y. Yang, and W. H. Matthaeus, Multipoint turbulence analysis with HelioSwarm, *Astrophys. J. Lett.* **945**, L20 (2023).

- [32] J. L. Burch, T. E. Moore, R. B. Torbert, and B. L. Giles, Magnetospheric multiscale overview and science objectives, *Space Sci. Rev.* **199**, 5 (2016).
- [33] C. T. Russell *et al.*, The magnetospheric multiscale magnetometers, *Space Sci. Rev.* **199**, 189 (2016).
- [34] C. Pollock *et al.*, Fast plasma investigation for magnetospheric multiscale, *Space Sci. Rev.* **199**, 331 (2016).
- [35] Y. Yang, F. Pecora, W. H. Matthaeus, S. Roy, M. E. Cuesta, A. Chasapis, T. Parashar, R. Bandyopadhyay, D. J. Gershman, B. L. Giles, and J. L. Burch, Quantifying the agyrotropy of proton and electron heating in turbulent plasmas, *Astrophys. J.* **944**, 148 (2023).
- [36] W. H. Matthaeus, C. W. Smith, and J. W. Bieber, Correlation lengths, the ultrascale, and the spatial structure of interplanetary turbulence, *AIP Conf. Proc.* **471**, 511 (1999).
- [37] M. W. Dunlop, A. Balogh, K.-H. Glassmeier, and P. Robert, Four-point cluster application of magnetic field analysis tools: The curlometer, *J. Geophys. Res.* **107**, 23 (2002).
- [38] G. Paschmann and P. W. Daly, Analysis Methods for Multi-Spacecraft Data, ISSI Scientific Reports Series SR-001, ESA/ISSI, 1998.
- [39] <https://hpde.io/NASA/NumericalData/MMS>.
- [40] L. Z. Hadid, F. Sahraoui, S. Galtier, and S. Y. Huang, Compressible magnetohydrodynamic turbulence in the earth's magnetosheath: Estimation of the energy cascade rate using *in situ* spacecraft data, *Phys. Rev. Lett.* **120**, 055102 (2018).
- [41] N. Andrés, F. Sahraoui, S. Galtier, L. Z. Hadid, R. Ferrand, and S. Y. Huang, Energy cascade rate measured in a collisionless space plasma with MMS data and compressible Hall magnetohydrodynamic turbulence theory, *Phys. Rev. Lett.* **123**, 245101 (2019).
- [42] N. Andrés, F. Sahraoui, S. Galtier, L. Z. Hadid, P. Dmitruk, and P. D. Mininni, Energy cascade rate in isothermal compressible magnetohydrodynamic turbulence, *J. Plasma Phys.* **84**, 905840404 (2018).
- [43] M. L. Goldstein, P. Escoubet, K.-J. Hwang, D. E. Wendel, A.-F. Viñas, S. F. Fung, S. Perri, S. Servidio, J. S. Pickett, G. K. Parks *et al.*, Multipoint observations of plasma phenomena made in space by cluster, *J. Plasma Phys.* **81**, 325810301 (2015).
- [44] H. E. Spence, HelioSwarm: Unlocking the multiscale mysteries of weakly-collisional magnetized plasma turbulence and ion heating, in *AGU Fall Meeting Abstracts* (2019), Vol. 2019, pp. SH11B-04.
- [45] K. G. Klein *et al.*, HelioSwarm: A multipoint, multiscale mission to characterize turbulence, *Space Sci. Rev.* **219**, 74 (2023).
- [46] A. Retinò *et al.*, Particle energization in space plasmas: Towards a multi-point, multi-scale plasma observatory, *Exp. Astron.* **54**, 427 (2022).